

Optimum Design of Active and Passive Cable Stayed Footbridges

F.L.S. Ferreira¹ and L.M.C. Simoes²

¹Department of Civil Engineering
University of Oporto, Portugal

²Department of Civil Engineering
University of Coimbra, Portugal

Abstract

In the last decades there is an increasing interest and investigation in the area of control applied to civil engineering structures. It's been shown that it is possible to improve structural performance by providing control devices that use sensors information to modify the dynamic properties.

An integrated cable-stayed bridge and control strategy system is designed in view of improving safety against dynamic loading, in particular pedestrian vibration.

The design problem concerns the optimization with goals of minimum cost, stresses, accelerations and displacements. It is cast as a multi-objective optimization and a Pareto solution is sought. An entropy-based technique is used to find the minimax solution by minimizing a convex scalar function.

Keywords: cable stayed, structural control, multi-objective optimization, integrated design.

1 Introduction

Traditionally, structures and their control devices are designed separately. An integrated optimum design is proposed here for a cable stayed pedestrian bridge.

Tzan and Pantelides [1] presented a methodology to optimally design an active frame subject to seismic excitation, the objective being minimize the structural volume with constraints of story drift and stresses. Khot [2] proposed an approach to optimally design integrated space systems using multi-objective optimization with goals of minimum volume, control force and time to suppress oscillations. In 2008 Cimellaro *et al.* [3] illustrated a two-stage optimization procedure for designing active steel frames. In 2009 Cimellaro *et al.* [4] extended their work to account for inelastic structures.

Steel footbridges are usually very flexible structures this, added to their low inherent damping, amplifies their response under dynamic loading. SETRA [5] published a

comprehensive guide for the design of such structures highlighting the importance of their dynamic properties.

The steel footbridge presented here is intended to guarantee serviceability along running events such as a marathon. Only vertical vibrations are accounted so a two dimensional model is used. The objective is to find two different optimum solutions associated with passive and active bridges. The current European regulation, EC0 [6] and EC1 Part1-2 [7] are employed.

The design technique uses a multi-objective optimization format with goal of minimum cost, stresses, deflections, accelerations and a Pareto solution is sought. An entropy-based methodology is used to determine the minimax solution by the minimization of a convex scalar function.

2 Problem formulation

2.1 Model Description

The footbridge has a total of 70m span and it is located 6m above ground foundation (Figure 1). It is assumed to be 6m wide for pedestrian crossing. A non symmetric geometry is adopted with 3 and 2 passive cables respectively in the left and right span for the active design and 4 and 2 in the passive design.

It is assumed that the foundation is sufficiently stiff to neglect the soil-structure interaction. The right span abutment restricts the horizontal movements of the deck. The tower/deck connection restricts the horizontal movements, the vertical connection properties are considered as design variables (Figure 2).

The footbridge is totally made of steel. The deck is made of a concrete slab which is disconnected from the supporting profile. The bridge is controlled using a single active tendon (AT).

It is used an HEB profile for the deck with different heights in the left and right span. The tower uses a rectangular hollow section (RHS).

The structure is made in steel class S275. The cables maximum stress is considered 700MPa and the active cable has a maximum tension of 1200kN.

The cost was considered to be 11000€/m³ for the deck steel, 15000€/m³ for the tower steel, 20000€/m³ for cable steel and 500€/m³ for the concrete slab.

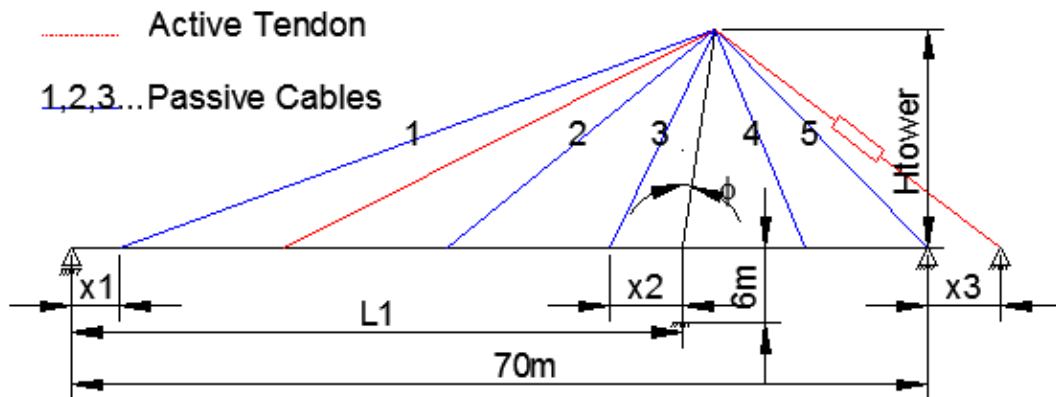


Figure 1: Bridge geometry

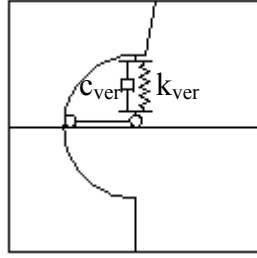


Figure 2: Tower Deck connection

The geometrical properties of the HEB profiles are determined using a polynomial regression model. This regression model allows the use of continuous and differentiable functions for the area and inertia properties. The area is determined using a 6th degree polynomial fit. To account for the large variation, the inertia fit was determined using the regression in Equation (1). The maximum error of this regression is 4% for the area fit and 3% for the inertia fit.

$$I_{HEB} = e^{6^{th} \text{ degree polynomial } (h_{HEB})} \quad (\text{eq. 1})$$

2.2 Design Variables

A total of 29 design variables (DV) described in Table 1 are considered even if the passive design does not account for the active control DV.

DV nº	Description	DV nº	Description
1	Bridge left span (L1)	16	Prestress of the 1 st cable
2	First anchorage (x1)	17	Prestress of the 2 nd cable
3	Last anchorage (x2)	18	Prestress of the 3 rd cable
4	Tower height (Htower)	19	Prestress of the 4 th cable
5	HEB height in left span	20	Prestress of the 5 th cable
6	HEB height in right span	21	Prestress of the 6 th cable
7	Base RHS height	21	Prestress of the AT (T_0^{AT})
8	Base RHS width	22	k_1 of the active control
9	Base RHS thickness	23	k_2 of the active control
10	Tower RHS height	24	Concrete slab height
11	Tower RHS width	25	Vertical connection stiffness (k_{ver})
12	Tower RHS thickness	26	Tower angle (ϕ)
13	Left span cables area	27	c_1 of the active control
14	Right span cables area	28	c_2 of the active control
15	Active tendon anchorage (x3)	29	Vertical connection damping (c_{ver})

Table 1: Problem design variables

2.3 Static Design

The 4 loadings types are: Self weight “G_k”; Imposed load “Q_k=5kN/m²”; Wind “W_k=1kN/m²”; and cables prestress “P”. The corresponding reduction and combination factors can be taken from the EC0 [5].

For the design 6 loading cases are considered (Table 2), 3 for service limit states (SLS) and 3 for ultimate limit states (ULS).

<i>Nomenclature</i>	<i>Design action combination</i>	<i>Span arrangement</i>
SLS-1	“G _k ”+”P”	-
SLS-2	“G _k ”+”P”+0.2”W _k ”+ 0.3”Q _k ”	Figure 3 a)
SLS-3	“G _k ”+”P”+0.5”Q _k ”+0”W _k ”	Figure 3 b)
ULS-1	“G _k ”+1.15”P”+1.5”W _k ”+ 1.5*0.7”Q _k ”	Figure 3 a)
ULS-2	1.35“G _k ”+0.85”P”+1.5”Q _k ”+ 1.5*0.6”W _k ”	Figure 3 b)
ULS-3	1.35“G _k ”+”P”+1.5”Q _k ”+ 1.5*0.6”W _k ”	Figure 3 c)

Table 2: Design combination

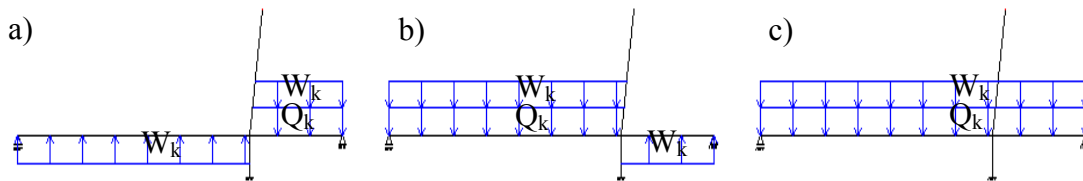


Figure 3: Loading conditions

The state variables (SV) are given in Table 3. In the optimization algorithm all of them are divided by their limit value. The goal will be to find the optimum cost structure having all SV within it's given limits (safety factor under 1).

<i>Design restriction</i>	<i>Combination utilized</i>	<i>Limit values</i>
Deck Stress	ULS-1,2 and 3	Elastic limit
Tower Stress	ULS-1,2 and 3	Elastic and buckling limit
Cable Tension	ULS-1,2 and 3	Between 15 and 100% of the limit elastic stress
Active Cable Tension	SLS-1	Between 240 and 960 kN
Active Cable Tension	ULS-1,2 and 3	Between 180 and 1200 kN
Tower and Deck Displacement	SLS-1	L/1500 limit for displacements
Tower and Deck Displacement	SLS-2 and 3	L/500 limit for displacements

Table 3: Static state variables

2.4 Dynamic Design

The footbridge is intended to allow its crossing along a running event. It must have deflections and accelerations under the allowable comfort range. Therefore the comfort level should be set to the minimum. The dynamic SV and their corresponding limit are given in Table 4.

<i>Design restriction</i>	<i>Limit values</i>
Deck and tower acceleration	2.5 m/s ²
Active Cable Tension increment	120 kN
Tower and Deck Displacement	L/500 limit for displacements
Passive damper force	30kN

Table 4: Dynamic state variables

The dynamic design scenario consists in crowd of runner's with a density d of 1 runner/m², velocity of 4.5 m/s and frequency between 2 and 4 Hz. The design considers a crowd pacing rate of 2, 2.5, 3, 3.5, 4Hz and also with a pacing rate coincident with the natural frequencies of the bridge in the same interval.

The dynamic loading of runners is characterized by its frequency after that the remaining properties and the time history loading can be defined [5]:

1. The quotient between the peak force and the static weight of the runner $-kp$;
2. The contact time of the pace $-tp$.

After defining the frequency the time history loading can be determined (Figure 4).

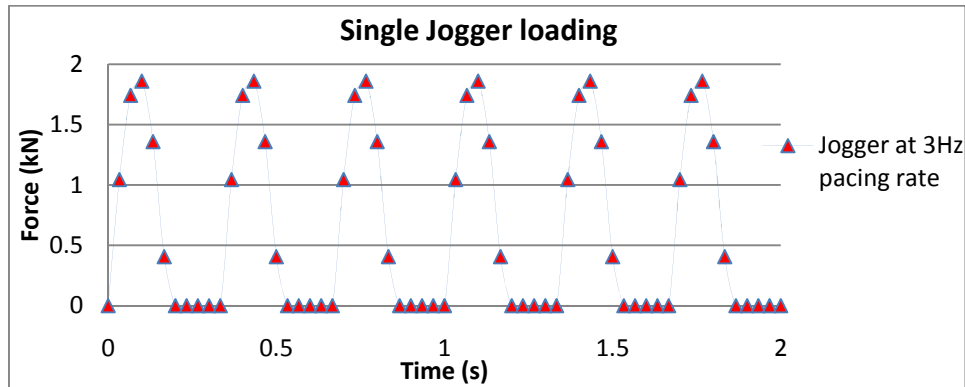


Figure 4: Time history loading of a single jogger

The runners are modelled as a series of moving loads with the prescribed time history loading. For design purposes it is assumed all joggers are at the same frequency with random phase. For the analysis the equivalent number of pedestrians all the same frequency (N_{eq}) is evaluated (eq 3) all at the same frequency using the total number of pedestrians N (eq 2).

$$N = d \times span \times wide = 420 \text{ runners} \quad (\text{eq. 2})$$

$$N_{eq} = 1.85 \times \sqrt{N} \approx 38 \text{ runners} \quad (\text{eq. 3})$$

2.5 Passive damper and Active Tendon Control

The active tendon uses information provided by the sensors at location 1 and 2 (Figure 5) giving displacement and velocity.

This active tendon induces an axial tension T^{AT} in its entire length (Figure 5) which is deflected in the top of the tower. The active tendon anchors in the deck and at a certain location outside the footbridge.

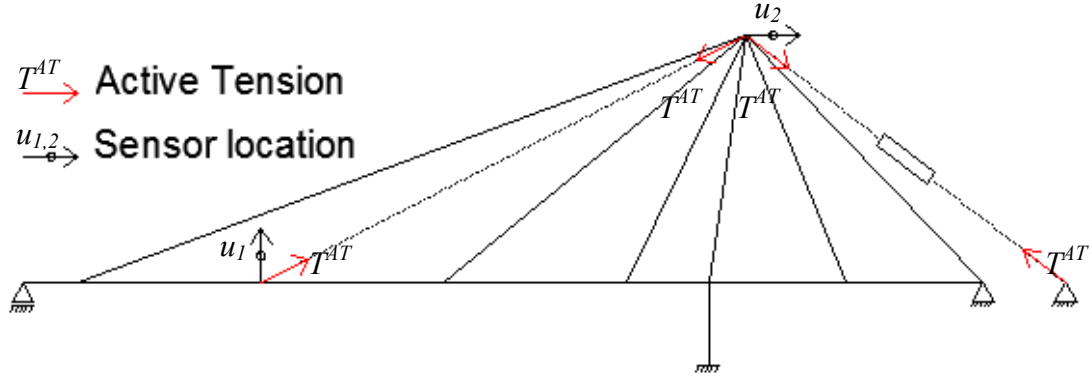


Figure 5: Sensor location and active tendon effect in the structure

The parameters of the control law were considered as design variables. In the initial solution a stable control system with added damping to the system was aimed. The control law is formulated in Equation (4).

$$T^{AT} = T_0^{AT} + [k_1 \quad k_2] \times \begin{bmatrix} u_1 \\ u_2 \end{bmatrix} + [c_1 \quad c_2] \times \begin{bmatrix} \dot{u}_1 \\ \dot{u}_2 \end{bmatrix} \quad (\text{eq. 4})$$

For modelling the matrices K^{AT} and C^{AT} were found, corresponding to the active tendon effect in the structure in terms of stiffness and damping respectively (eq. 5 to 8).

$$K^{AT} = -f_{un}^{AT} \times [0 \quad \dots \quad k_1 \quad \dots \quad k_2 \quad \dots] \quad (\text{eq. 5})$$

$$C^{AT} = -f_{un}^{AT} \times [0 \quad \dots \quad c_1 \quad \dots \quad c_2 \quad \dots] \quad (\text{eq. 6})$$

$$K^{structAT} = K^{struct} + K^{AT} \quad (\text{eq. 7})$$

$$C^{structAT} = C^{Rayleigh} + C^{AT} + C^{ver} \quad (\text{eq. 8})$$

Legend:

$K^{structAT}$	Structural stiffness matrix including active tendon effect
$C^{structAT}$	Structural damping matrix including active tendon effect
K^{struct}	Structural stiffness matrix
C^{ver}	Vertical restriction damping
f_{un}^{AT}	Active tendon unitary force

The inherent structural damping ($C^{Rayleigh}$) was obtained by using a Rayleigh damping matrix. A critical damping ξ of 0.4% was assigned for Frequencies of 2 and 4Hz (Figure 6). Since the frequencies of interest are in this range a conservative approach is followed. This approach has the added advantage of creating a damping sensitivity to the structural frequency, consequently the optimization algorithm will search for structural frequencies outside this low damped range. The real damping accounts the active cable and the vertical restriction effects.

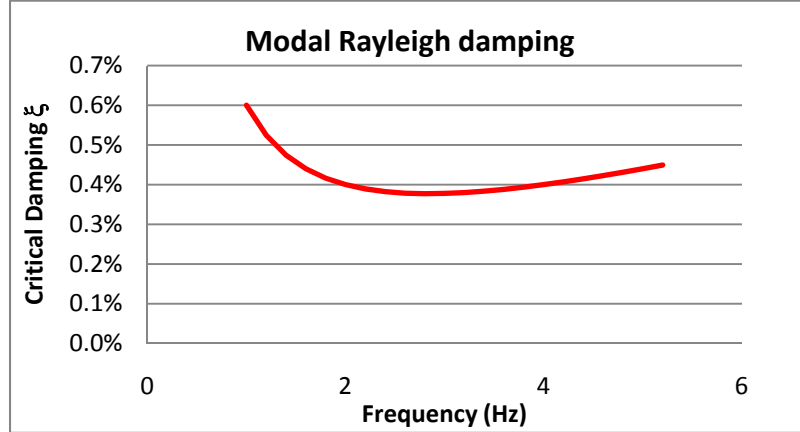


Figure 6: Rayleigh damping

3 Optimization strategy

3.1 Minimax objective function

The integrated optimum design is cast as a multiple objective optimization and a Pareto solution is sought. An entropy-based technique is used to find the minimax solution by minimizing a convex scalar problem. This is shown by minimum entropy principle, the problem being formulated as a Kreisselmeyer-Stainhauser scalar function [8]. This form leads to a convex approximation of the goals (eq. 9). Accuracy increases with ρ .

$$\text{Minimize } \frac{1}{\rho} \ln \left[\sum_{i=1}^{N_{SV}} e^{\rho \left[F^i(\bar{v}) + \sum_{j=1}^{N_{DV}} \left(\frac{\partial F^i(\bar{v})}{\partial v_j} \times \Delta v_j \right) - 1 \right]} \right] \quad (\text{eq. 9})$$

Legend:

- N_{SV} Number of state variables
- N_{DV} Number of design variables
- $F^i(\bar{v})$ State variable number i
- v_j Design variable number j
- Δv_j Design variable number j increment

3.2 Solution procedure

The static and dynamic state variables are always divided by their maximum value so the goal is to have all of them inferior to one. The reference cost is updated so the cost state variable is always equal to 1. If the structure doesn't comply with all design criteria the algorithm will aim for a suitable solution and once it is found the goal will be to reduce the cost keeping its integrity.

The optimization algorithm uses 131 State Variables under static conditions. For dynamic conditions a time history of each state variable must be considered. Therefore, if one uses the entire time history, a significant calculation time would be required to find the optimum DV increment. In order to improve calculation time by accepting a small loss off accuracy only n numbers of extreme values were retained. In this case $n=3$ was set, even if it is a small value it provides good results. This results in 936 state variables for dynamic loading.

In each iteration all the state variables are determined and their respective sensitivity using finite difference method. The output is a 1068 state variables vector and a 1068×29 gradient matrix. This output is introduced in the optimization algorithm which gives the optimum design variables changes. Design variables changes are limited in order to guarantee that the linearized approximation is accurate.

4 Results

4.1 Bridge design

The results of the optimized design of an active and passive bridge are given below. The passive bridge uses very similar geometry and substitutes the active tendon in the left span by a passive cable.

The optimization process can converge into two possible scenarios:

1. Unfeasible design with optimum safety factor superior to one;
2. Feasible design with safety factor equal to one and optimum cost.

For reasons concerning the characteristic of the problem the algorithm can only determine the local optimum design. Multi start approach is adopted in order to find the global maximum. The active bridge initial design was a modification of the passive bridge final design. It was not a suitable design for the active geometry but it converged to the best cost solution achieved.

4.1.1 Active Bridge

Table 5 presents the initial, optimum and the correspondent maximum and minimum values of the design variables in the active design. The values at bold converged to one of its limits.

<i>Design Variables</i>	<i>Initial DV</i>	<i>Final DV</i>	<i>Max DV</i>	<i>Min DV</i>	<i>Units</i>
Bridge left span (L1)	43,0	44,5	60	35	m
First anchorage (x1)	5,0	2,6	8	2	m
Last anchorage (x2)	5,2	8,0	8	3	m
Tower height (Htower)	13,3	11,2	30	10	m
HEB height in left span	0,65	HEB700	1	0,1	m
HEB height in right span	0,65	HEB450	1	0,1	m
Base RHS height	0,50	0,50	3	0,5	m
Base RHS width	1,0	1,0	4	1	m
Base RHS thickness	0,05	0,05	0,3	0,05	m
Tower RHS height	0,44	0,30	2	0,3	m
Tower RHS width	0,50	0,50	3	0,5	m
Tower RHS thickness	0,02	0,02	0,1	0,02	m
Left span cables area	15	12	100	7	cm ²
Right span cables area	24	15	100	10	cm ²
Active tendon anchorage (x3)	6,0	5,7	20	2	m
Prestress of the 1 st cable	367	400	400	50	kN
Prestress of the 2 nd cable	400	345	400	50	kN
Prestress of the 3 rd cable	264	261	400	50	kN
Prestress of the 4 th cable	800	533	1000	100	kN
Prestress of the 5 th cable	796	503	1000	100	kN
Prestress of the AT (T_0^{AT})	200	442	1000	100	kN
k_1 of the active control	-3000	-3617	-20000	-100	kN/m
k_2 of the active control	3000	1942	20000	-20000	kN/m
Concrete slab height	0,15	0,10	1	0,01	m
Vertical connection stiffness (k_{ver})	1000	2351	20000	10	kN/m
Tower angle (ϕ)	7,9	9,1	27	0	°
c_1 of the active control	-400	-360	-2000	-10	kNs/m
c_2 of the active control	-200	-202	-2000	2000	kNs/m

Table 5: Design variables

The geometry comparison of both designs can be seen in Figure 7. From the results it is observed that in the active bridge:

1. The tower was located in 2/3 of the span;
2. In the left span the cables anchored closer to the support;
3. The tower height decreased almost to the minimum value;
4. The HEB profile in the left span is higher than in the right span, this was not expected and was probably a consequence of the active cable topology option;
5. There is huge cross section reduction with the tower having its minimum value and cables reduced also;

6. The design determined the optimal stiffness of the tower/deck vertical connection. Under dynamic events the connection is considered rigid in this active geometry.
7. The control variables were modified in order to provide optimum damping and stiffness to the structure.

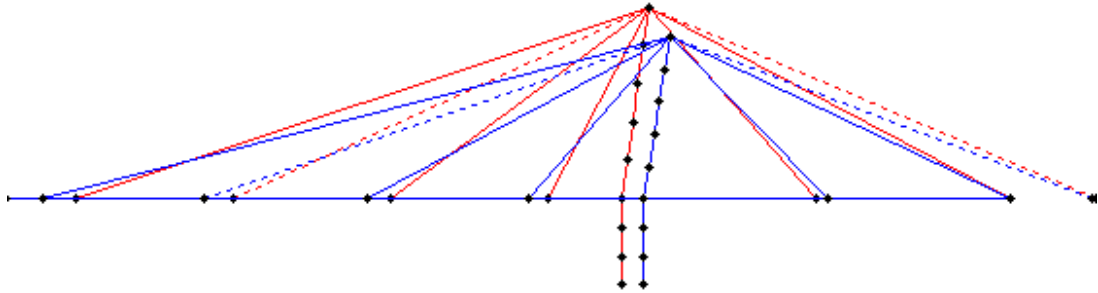


Figure 7: Comparison between the initial (red) and the optimum active bridge geometry (blue)

The iteration information is presented in Figure 8. It can be seen that the initial design is unsafe so at first a feasible design is searched with the consequent cost increase. After a safe scenario is found the goal is to improve the cost. Since there is a limitation in the choice of the HEB profile for the deck, after the 100th iteration the optimization algorithm is reinitiated with the profiles closer to the optimum determined ones. For this reason after the 100th iteration the cost increased a little before decreasing again. The optimal design costs 103.931€.

After a safe design is found some design iterations were unsafe. This can be explained by the linear approximation model and can easily be solved by reducing the maximum increment. Doing so increases the calculation time and does not bring significant improvements. There must be a compromise in the allowable increment in order to have efficiency and accuracy.

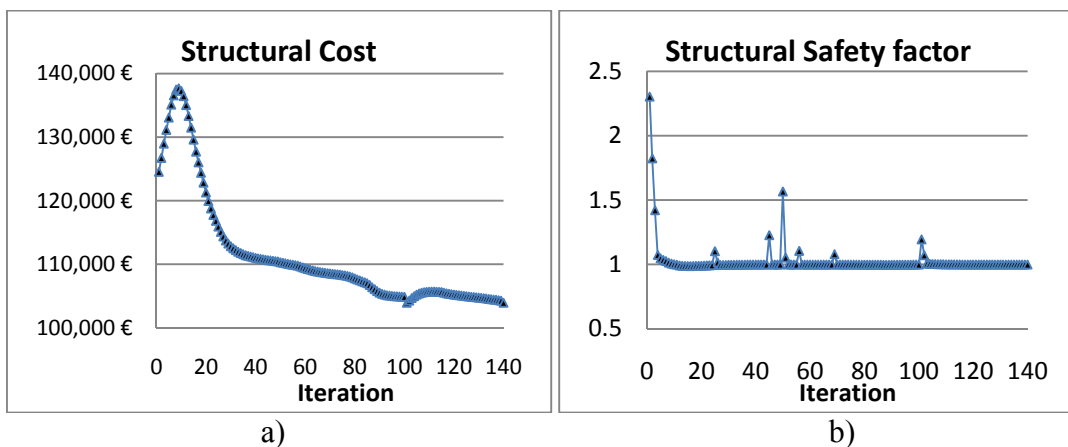


Figure 8: Active bridge iteration evolution throughout the optimization; a) Cost, b) Safety

The initial and optimum state variable vector can be seen in Figure 9. The values plotted are detailed in Tables 6 to 8 and Figures 10 and 11. The Figure 10 and 11 shows the results in the corresponding units. A deck acceleration of 2.5 m/s^2 corresponds to 1 in state variable units.

The initial design had several problems (marked at red). Cable 5 and active tendon were slack at ULS-1 with tension inferior to 15% of the maximum (Table 6). The tower had great displacement under the self weight of the structure (Table 8). There was also very high deck accelerations (Figure 10a) resulting from a low damped, 4.07 Hz frequency mode of vibration (Table 13).

Neither the tower accelerations (Figure 10b) nor active tendon force (Figure 11) were critical for the design.

The optimal design is reached when all the problems are solved and several state variables are very close to their limit (green).

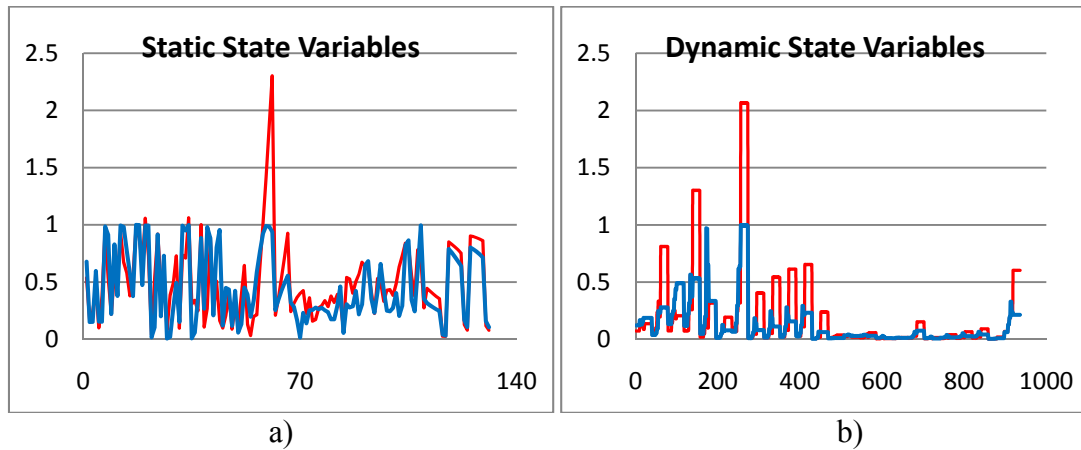


Figure 9: Active bridge state variables vector initial (red) and final (blue); a) Static, b) Dynamic

Cable number	<i>Initial</i>				<i>Final</i>			
	ULS-1	ULS-2	ULS-3	SLS-1	ULS-1	ULS-2	ULS-3	SLS-1
1	0,54	0,38	0,54	-	0,68	0,15	0,38	-
2	0,17	0,97	0,93	-	0,15	0,99	0,99	-
3	0,25	0,54	0,67	-	0,15	0,91	0,98	-
4	0,44	0,22	0,58	-	0,60	0,22	0,77	-
5	0,1	0,56	0,38	-	0,15	0,83	0,58	-
Active Tendon	0,1	0,74	0,71	0,2	0,15	0,99	0,95	0,71

Table 6: Active bridge cable tension SV

Zone	Initial			Final		
	ULS-1	ULS-2	ULS-3	ULS-1	ULS-2	ULS-3
Deck left span	0,393	0,674	0,84	0,291	0,683	0,865
Deck right span	0,331	0,501	0,701	0,461	0,659	0,996
Base tower	0,027	0,129	0,118	0,041	0,169	0,160
Tower	0,446	0,851	0,903	0,317	0,788	0,802

Table 7: Active bridge M-N interaction SV

Zone	Initial			Final		
	SLS-1	SLS-2	SLS-3	SLS-1	SLS-2	SLS-3
Deck left span	0,888	0,388	0,646	0,981	0,449	0,451
Deck right span	0,509	0,284	0,214	0,955	0,424	0,584
Base tower	2,303	0,927	0,426	0,991	0,556	0,319

Table 8: Active bridge displacement SV

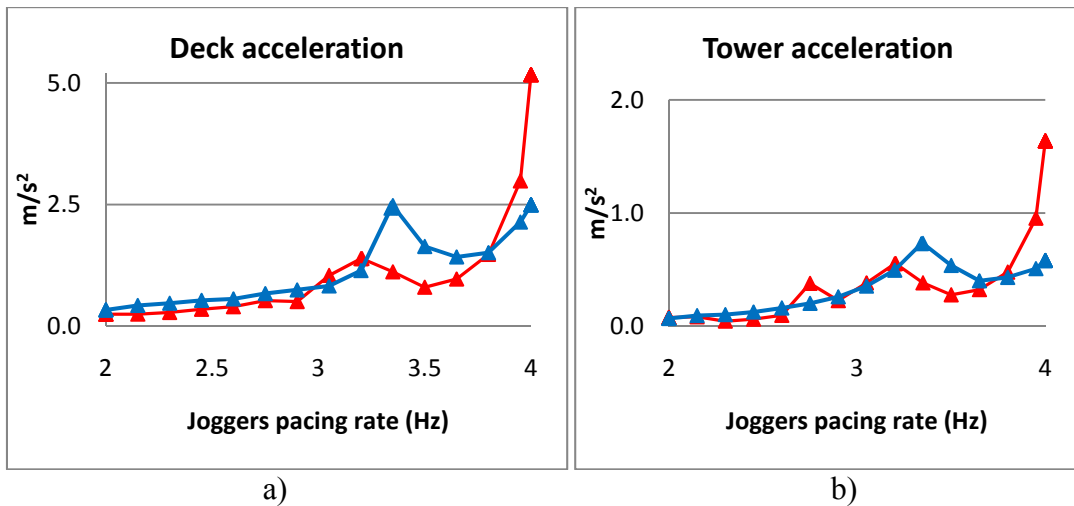


Figure 10: Active bridge initial (red) and final (blue) response vs joggers pacing rate; a) Deck acceleration, b) Tower acceleration

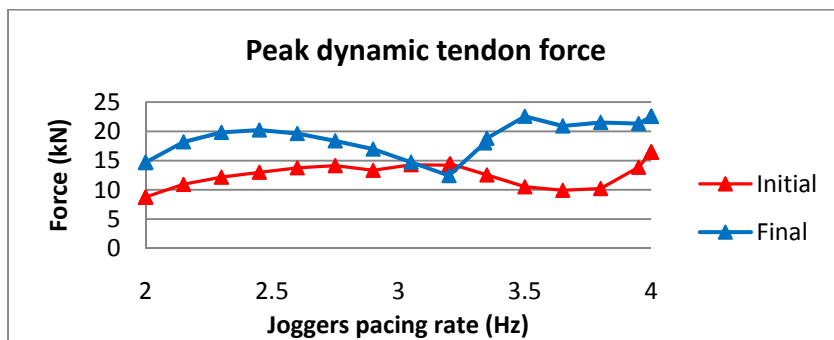


Figure 11: Active bridge Tendon force vs pacing rate

4.1.2 Passive Bridge

The approach was a little different for the passive bridge design. After examining several design possibilities it proved to be hard to find a solution that would grant deck accelerations lower than the established limit (2.5 m/s^2). Most of the multi-start initial design converged to unfeasible solution. The solution was to begin with a very heavy and costly structure, using very large cross sections and a concrete slab with 0.4m in order to guarantee low accelerations. The optimization algorithm was then in a better chance of finding a feasible optimum cost solution. The initial and optimum DV with their corresponding minimum and maximum values can be seen in Table 9. The values at bold converged to one of its limits.

<i>Design Variables</i>	<i>Initial DV</i>	<i>Final DV</i>	<i>Max DV</i>	<i>Min DV</i>	<i>Units</i>
Bridge left span (L1)	50	42,8	60	35	m
First anchorage (x1)	4	5,0	8	2	m
Last anchorage (x2)	6	5,2	8	3	m
Tower height (Htower)	18	13,2	30	10	m
HEB height in left span	0,7	HEB650	1	0,1	m
HEB height in right span	1	HEB650	1	0,1	m
Base RHS height	1,5	0,50	3	0,5	m
Base RHS width	3	1,0	4	1	m
Base RHS thickness	0,15	0,05	0,3	0,05	m
Tower RHS height	0,9	0,40	2	0,3	m
Tower RHS width	1,4	0,50	3	0,5	m
Tower RHS thickness	0,08	0,02	0,1	0,02	m
Left span cables area	60	15	100	7	cm ²
Right span cables area	90	23	100	10	cm ²
Prestress of the 1 st cable	600	363	400	50	kN
Prestress of the 2 nd cable	600	212	400	50	kN
Prestress of the 3 rd cable	600	400	400	50	kN
Prestress of the 4 th cable	600	238	1000	100	kN
Prestress of the 5 th cable	1000	800	1000	100	kN
Prestress of the 6 th cable	1000	775	1000	100	kN
Concrete slab height	0,4	0,15	1	0,01	m
Vertical connection stiffness (k_{ver})	1000	1075	20000	10	kN/m
Tower angle (ϕ)	8,6	7,9	27	0	°
Vertical connection damping (c_{ver})	50	65	40000	1	kNs/m

Table 9: Design Variables

The geometry comparison of both designs can be seen in Figure 12. From the results for the passive bridge stems:

1. The tower is located in 2/3 of the span;
2. The tower height decreased significantly;
3. The HEB profile in the left span is the same as in the right span;
4. We see huge cross section reduction in the tower and cables;
5. The concrete slab reduced from 40 to 15cm;
6. The algorithm improved the dynamic properties so that the tower/deck vertical restriction could provide optimum damping and stiffness;

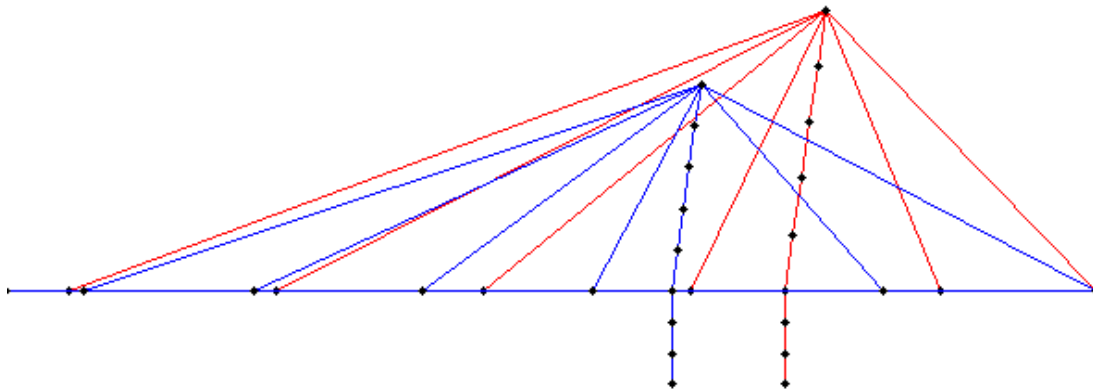


Figure 12: Comparison between the passive bridge initial (red) and the optimum geometry (blue)

The iteration information is presented in Figure 13. It can be seen that the initial solution even though high costly doesn't comply with the design criteria. There is a cost increase and after a suitable solution is found the cost drops drastically. Since the cost was already in a descending branch after 100 iterations the optimization process continued further one until the 140th iteration. After that the algorithm was reinitiated with the profiles restricted for 40 iterations. The optimal design costs 125.160€.

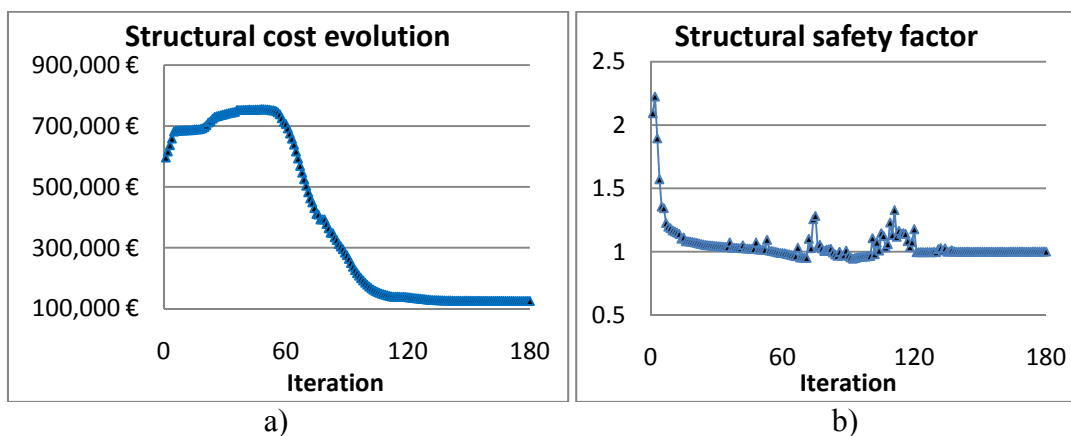


Figure 13: Passive bridge iteration evolution throughout the optimization; a) Cost, b) Safety

The initial and optimum state variable (SV) vector can be seen in Figure 14. The values are detailed in Tables 10 to 12 and Figures 15 and 16. The initial design consisted in a very heavy bridge with 0.4m concrete slab.

The initial design had several problems (marked at red). The cables were slack because of their high cross section (Table 10). There were high stresses and displacements in the deck left span (Table 11 and 12). The optimum design managed to solve these problems and maintain the accelerations within the allowable limit (Figure 15a). This was possible due to the correct dimensioning of the passive damper which damped several modes (Table 13). Neither the tower accelerations (Figure 15b) nor passive damper force (Figure 16) were critical for the design.

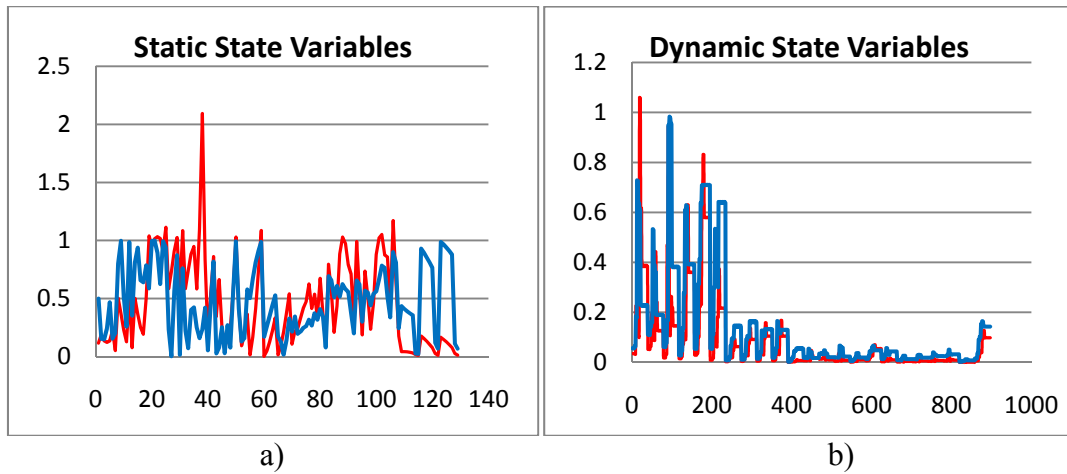


Figure 14: Passive bridge state variables vector initial (red) and final (blue); a) Static, b) Dynamic

Cable number	<i>Initial</i>			<i>Final</i>		
	ULS-1	ULS-2	ULS-3	ULS-1	ULS-2	ULS-3
1	0,12	0,05	0,08	0,50	0,20	0,35
2	0,19	0,50	0,50	0,15	0,80	0,81
3	0,14	0,37	0,37	0,15	1,00	0,94
4	0,12	0,23	0,25	0,24	0,52	0,66
5	0,14	0,13	0,19	0,47	0,26	0,64
6	0,22	0,52	0,50	0,16	0,99	0,79

Table 10: Passive bridge cable tension

Zone	<i>Initial</i>			<i>Final</i>		
	ULS-1	ULS-2	ULS-3	ULS-1	ULS-2	ULS-3
Deck left span	0,675	1,030	1,172	0,41	0,69	0,90
Deck right span	0,369	0,562	0,653	0,34	0,62	0,81
Base tower	0,018	0,027	0,028	0,03	0,12	0,11
Tower	0,043	0,176	0,167	0,43	0,93	0,99

Table 11: Passive bridge M-N interaction

Zone	Initial			Final		
	SLS-1	SLS-2	SLS-3	SLS-1	SLS-2	SLS-3
Deck left span	2,093	0,663	1,029	0,42	0,25	0,99
Deck right span	0,861	0,254	0,366	0,82	0,27	0,58
Tower	1,086	0,333	0,541	0,99	0,53	0,33

Table 12: Passive bridge static displacement

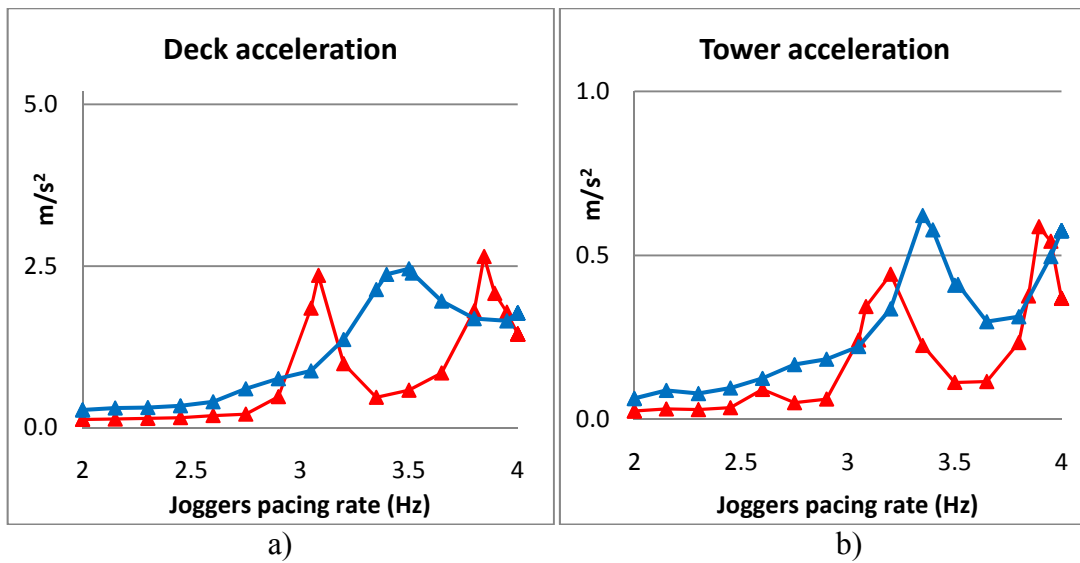


Figure 15: Passive bridge initial (red) and final (blue) response vs joggers pacing rate; a) Deck acceleration, b) Tower acceleration

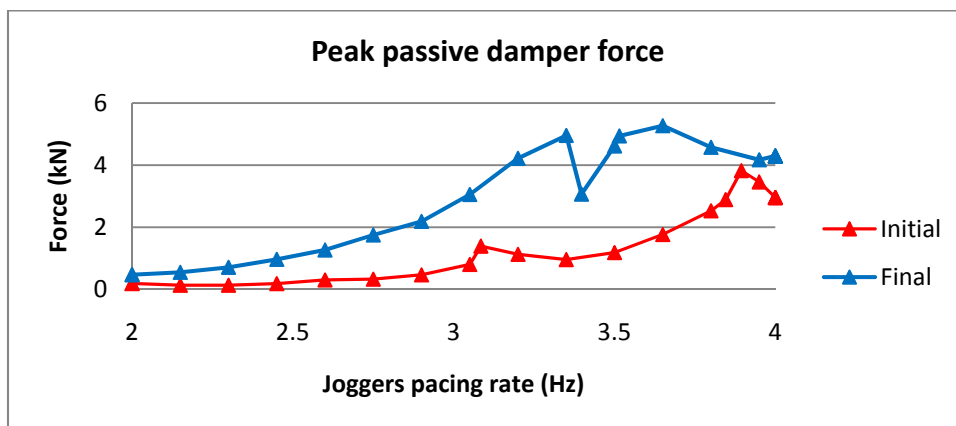


Figure 16: Passive bridge peak damper force

4.1.3 Active vs passive footbridge

The comparison of both optimum geometries can be seen Figure 17. The active bridge is slender with lower tower height. The active bridge tower is located to the right of the passive one but this can be explained by the design option to anchor the active tendon outside the bridge.

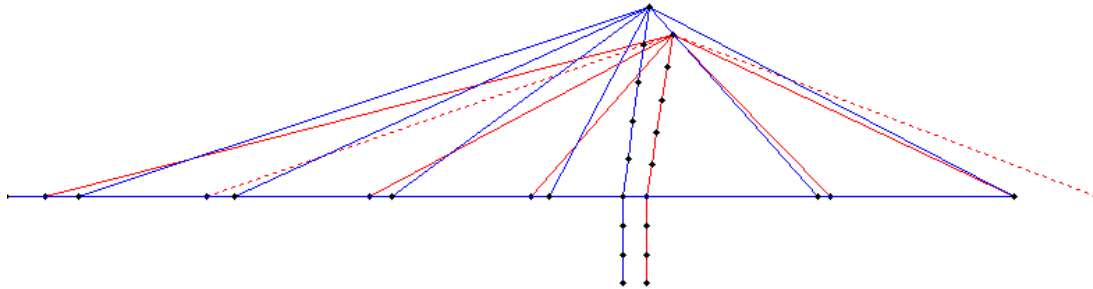


Figure 17: Comparison between both optimum geometries active (red) and passive (blue)

The dynamic performance of the bridge was a critical condition of the design. The main focus was to control the deck accelerations. There are two main ways of achieving the design criteria, one is to increase mass (added cost and weight) and the other is to add damping into the system. In both designs the correct dimensioning of protection devices introduced significant damping into the system. Table 13 resumes the frequencies f and damping factors ξ of both designs. A state space eigenvalue analysis was required in order to determine these properties.

Mode	Active Bridge				Passive Bridge			
	Initial		Optimum		Initial		Optimum	
	f	ξ	f	ξ	f	ξ	f	ξ
1	1,63	37%	1,86	25%	1,52	0,50%	1,52	0,50%
2	3,2	1,70%	3,34	5,40%	3,08	0,50%	3,4	2,60%
3	4,07	0,80%	4,24	3,30%	3,85	0,70%	3,52	6,40%
4	5,44	4,50%	6,77	2,00%	3,89	3,30%	4,18	1,60%
5	8,23	2,30%	8,94	0,80%	6,48	0,50%	5,62	0,50%
6	8,53	2,60%	11,3	1,30%	7,83	0,80%	8,12	0,70%

Table 13: Dynamic properties with and without AT

Figure 18 represent the passive and active bridge modes of vibration. They were obtained by considering not only the stiffness and mass matrix but also the damping, in consequence the eigenvalues have imaginary part. The most important contribution is represented.

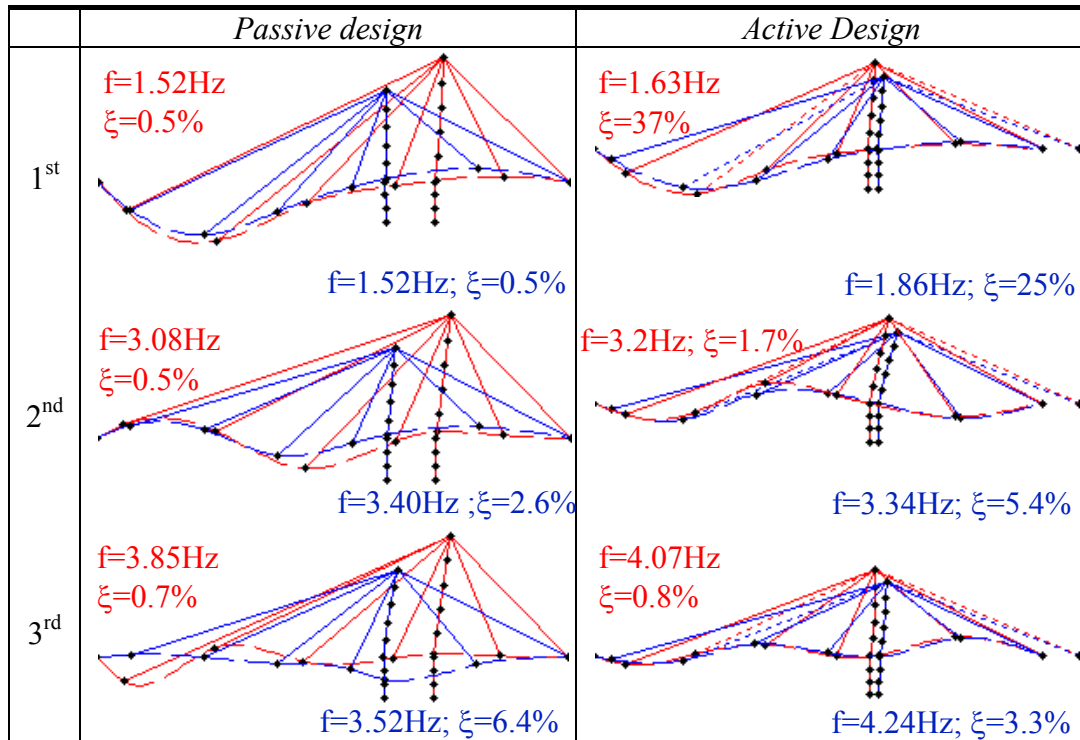


Figure 18: Passive and active bridge modes of vibration initial (red), final (blue)

5 Conclusions

This paper presents an algorithm to find the optimum design of a cable stayed footbridge including both passive and active protection devices. The methodology shows how such complex problem can be dealt efficiently. In the active structure the choice of the control variables could converge to an unstable design. The algorithm gives the control parameters that could change structural frequencies and add damping into the structure. In the passive structure the optimum damping coefficient of the connection has a convex evolution. If a low value is found no damping will be added, with a high value the frequencies increase but again no damping will be added. The algorithm was efficient in finding a compromise in the coefficient able to damp several modes.

Nonetheless because of the problems nature one is only able to ensure that a local minimum is found. For this reason a multi-start approach is employed.

The cost of the passive footbridge was 17% higher than in the active bridge design. The active bridge would be a viable solution if the active tendon initial plus operating cost don't exceed this cost difference (21.229€ here).

The active tendon is mainly designed to dissipate energy. The maximum power dissipated by the active tendon is 955W. Nonetheless sometimes it introduces energy into the structure, the peak power required by the active tendon is 106W and the average power is 4W. The active tendon has very low power consumption.

References

- [1] Tzan SR, Pantelides CP. Convex model for seismic design of structures—II: Design of conventional and active structures. *Earthquake Engineering & Structural Dynamics* 1996; 25:945–963.
- [2] Khot NS. Multicriteria optimization for design of structures with active control. *Journal of Aerospace Engineering (ASCE)* 1998; 11(2):45–51.
- [3] Cimellaro GP, Soong TT, Reinhorn AM. Invited paper: optimal integrated design of controlled structures. Third International Conference CIMTEC 2008 S.M.A.R.T. Materials Structures Systems, Acireale, Sicily, Italy, 8–13 June 2008.
- [4] Cimellaro GP, Soong TT, Reinhorn AM. Integrated design of inelastic controlled structural systems. *Structural Control and Health Monitoring* 2009; 16:689–702
- [5] SETRA/AFGC, *Footbridges – Assessment of dynamic behaviour under the action of pedestrians*, Guidelines. Sétra, March 2006.
- [6] EN 1990, *Eurocode 0 – Basis of structural design*. European Committee for Standardization, 2002.
- [7] EN 1991-2, *Eurocode 1– Actions on structures, Part 2: Traffic loads on bridges*. European Committee for Standardization, 2002.
- [8] Simões, L.M.C. and Templeman A.B. 1984, *Entropy Based Optimization of Cable Net Structures*. *Journal of Engineering Optimization* 1984, Vol 15, pp 120-140.